

BBA 32182

## Quarter field resonance and integer-spin/half-spin interaction in the EPR of *Thermus thermophilus* ferredoxin. Possible new fingerprints for three iron clusters

Wilfred R. Hagen<sup>a,\*</sup>, William R. Dunham<sup>a,\*\*</sup>, Michael K. Johnson<sup>b</sup> and James A. Fee<sup>a,\*\*\*</sup>

<sup>a</sup> Biophysics Research Division, The University of Michigan, 2200 Bonisteel Blvd., Ann Arbor, MI 48109 and <sup>b</sup> Department of Chemistry, Louisiana State University, Baton Rouge, LA 70803 (U.S.A.)

(Received October 2nd, 1984)

Key words: ESR; Ferredoxin; Iron-sulfur cluster; (*T. thermophilus*)

We describe two new characteristics of the EPR of the seven-iron containing ferredoxin from *Thermus thermophilus*. First, the reduced state of the 3Fe center, which has traditionally been considered to be EPR-silent, has been found to exhibit a  $\Delta m = 4$  transition, which is unique for Fe-S centers. This signal is similar to that of high-spin  $\text{Fe}^{2+}$ -EDTA and supports the suggestion that the ground electronic state of the 3Fe cluster is  $S = 2$ . Second, we have recorded the EPR spectrum of the fully reduced protein at 9 and 15 GHz and found that changes occur in the signal which are consistent with a weak electronic spin-spin interaction between the  $[\text{4Fe-4S}]^+$  ( $S = 1/2$ ) and the reduced 3Fe center. A theoretical explanation is given for the observation of interaction signals with constant effective  $g$  values.

### Introduction

Spin-coupling occurs between the individual Fe atoms of iron-sulfur clusters to give a resultant or system spin, the magnitude of which depends on the spin configuration of the individual atoms, the number of atoms in the cluster, and the oxidation state of the cluster. For example, the resultant spin of the oxidized [2Fe-2S] cluster is  $S = 0$ , whereas the system spin of the reduced cluster is  $S = 1/2$ . Such assignments are consistent with the early observation that only reduced ferredoxins exhibit

an EPR spectrum (cf. Refs. 1 and 2 for review). In the case of [4Fe-4S] clusters, which have three accessible oxidation states [3], there are three observed resultant spin states:  $S = 1/2$  from  $[\text{4Fe-4S}]^{3+}$ ,  $S = 0$  from  $[\text{4Fe-4S}]^{2+}$ , and  $S = 1/2$  from  $[\text{4Fe-4S}]^{1+}$  [4]. Recently, [3Fe- $n$ S] clusters have been discovered [4–6] which have electronic properties unlike those of either 2Fe or 4Fe systems. The oxidized state of these clusters exhibits an EPR signal near  $g = 2$  while the reduced form has generally been found to be EPR silent. Kent et al. [7] described an electronic model for the oxidized 3Fe cluster in which three high-spin  $\text{Fe}^{3+}$  were spin-coupled to give resultant  $S = 1/2$  in the oxidized form. The model suggested that the individual iron atoms within the cluster were in environments very much like that of the iron in rubredoxin, and a spin-coupling arrangement was imagined which accounted for the very different

\* Present address: Laboratory of Biochemistry, Agricultural University, De Dreijen 11, 6703 BC Wageningen, The Netherlands.

\*\* To whom correspondence should be addressed.

\*\*\* Present address: Division of Isotope and Nuclear Chemistry, Los Alamos National Laboratory, University of California, Los Alamos, NM 87545, U.S.A.

hyperfine coupling constants extracted from the Mössbauer spectrum [4,6]. The spin-coupling patterns in the reduced cluster are not yet defined, but Kent et al. [7] suggested that the system spin is integer,  $S > 1$ . From the temperature dependence of magnetic circular dichroism (MCD) spectra, Thomson et al. [8] tentatively concluded that  $S = 2$ . In this communication, we show that a weak EPR signal can be observed from the reduced three-iron cluster, and we believe this originates from an  $S = 2$  spin manifold.

Stout and his co-workers [5,9] have shown that the distances between the Fe clusters in 7Fe ferredoxins are not greatly different from those observed earlier in 8Fe ferredoxins [10]. Thus, the center-to-center distance is 12 Å in both the 7Fe protein from *Azotobacter vinelandii* [9] and the 8Fe protein from *Peptococcus aerogenes* [10]. Since spin-spin interactions have been shown to occur between the two  $[4\text{Fe-4S}]^{1+}$  clusters in *P. aerogenes* [11] and other ferredoxins [12], it is likely that spin-spin interactions will also occur between the reduced, paramagnetic clusters of 7Fe ferredoxins.

## Materials and Methods

*T. thermophilus* was grown as described by Findling et al. [13] and 7Fe ferredoxin was purified from cytosol as described by Hille et al. [14]. The material used in this study had a purity index of approx. 0.62 (cf. Ref. 14). Concentrated solutions of  $\text{Fe}^{2+}$ -EDTA were prepared under anaerobic conditions. All other materials were of the best available quality.

EPR spectra were recorded at X-band frequency with a Varian model E-112 system equipped with a homebuilt flow cryogenic system. EPR spectra recorded at P-band were recorded with a homebuilt instrument (cf. Ref. 15).

## Results and Discussion

As presented in Fig. 1, oxidized *Thermus* ferredoxin shows the EPR signal characteristic of 3Fe clusters as typified by a sharp peak at an effective  $g$  value slightly above 2 and a relatively structureless, broad feature at higher field. To characterize such a system in terms of its  $g$  values is possible

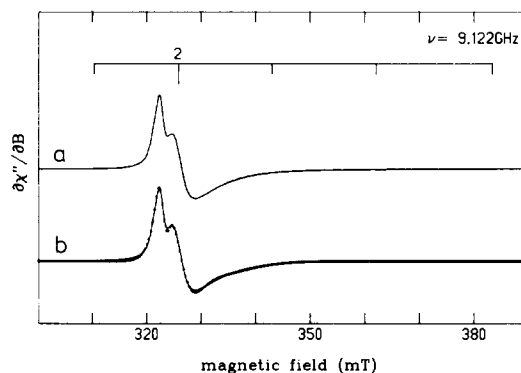


Fig. 1. The EPR spectrum of oxidized ferredoxin from *T. thermophilus* in 30% glycerol. The signal resulting from the oxidized protein shows increased resolution in the presence of the organic solvent. The data of spectrum a are duplicated in spectrum b and overlaid by a simulation (dots), assuming a single  $S = 1/2$  system exhibiting  $g$ -strain. Conditions of recording: protein concentration, 1.8 mM; microwave frequency, 9122 MHz; microwave power, 0.5 mW; modulation amplitude, 100 kHz; temperature, 12 K. Simulation parameters:  $g_{1,2,3} = 1.9358, 1.9923, 2.0239$ ;  $\Delta g_{11,22,33,12,13,23} = 0.0386, 0.0122, 0.0075, 0.0033, -0.0117, -0.0065$ .

only by simulating the spectral shape accurately using a computer program. Ohnishi et al. [16] have reported the parameters resulting from such a simulation but do not show the actual fit. In preparing *Thermus* ferredoxin for low-temperature magnetic circular dichroism experiments, we noticed that the EPR spectrum undergoes a significant sharpening upon dilution to 30% glycerol. We have analyzed this better-resolved signal using the recently developed statistical theory of  $g$  strain [17,18], and the resulting simulated spectrum is compared to the experimental spectrum in Fig. 1. The  $g$  values used were 2.024, 1.992, and 1.936; these are comparable to those reported earlier [16]. From the quality of this fit, based on the assumption of a single,  $g$ -strained  $S = 1/2$  system, it follows that the protein is homogeneous as observed from the site of the oxidized 3Fe center, and that multiple conformations (vide infra), with the exception of microconformations that show up as  $g$  strain, do not occur.

Other than the signal just described, the oxidized protein shows no EPR signals of significant intensity. Upon reduction with one electron equivalent, the signal of the oxidized protein is reduced to less than 2% of its original intensity [14] and, concom-

itantly, an extremely broad and weak signal appears at low field as shown in spectra a and c of Fig. 2. This signal is similar to the  $\Delta M = 4$  transition previously observed with high-spin ( $S = 2$ )  $\text{Fe}^{2+}$ -EDTA [19] shown here in spectra b and d of Fig. 2. When the potential of the solution is decreased by adding more dithionite, this broad signal increases its intensity slightly, and another EPR signal arising from the reduced 4Fe cluster appears [14,16].

The broad signal from the partially reduced ferredoxin very closely resembles that of  $\text{Fe}^{2+}$ -EDTA [19,20]. Previously, we were unable to simulate exactly the signal from  $\text{Fe}^{2+}$ -EDTA with simple perturbation theory [19], and this is also true for the ferredoxin signal. For the moment we

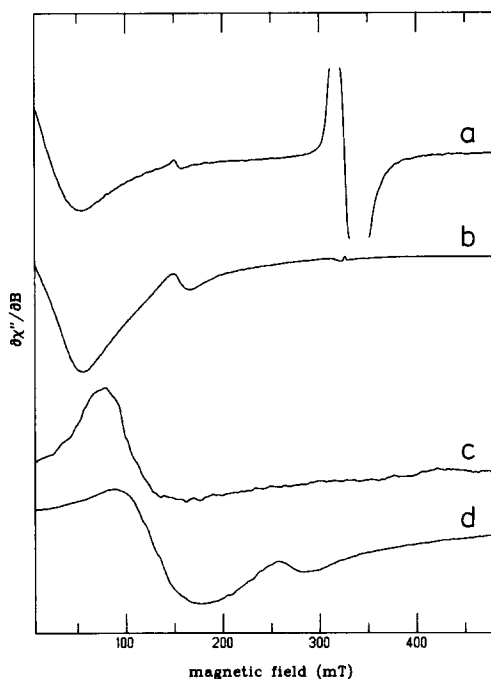


Fig. 2. Demonstration of the  $\Delta M = 4$  signal in partially reduced ferredoxin from *T. thermophilus* and in  $\text{Fe}^{2+}$ -EDTA. Spectrum a is the X-band spectrum of 1.8 mM half-reduced ferredoxin. The signal from the oxidized protein around  $g = 2$  corresponds to approx. 1% that of fully oxidized protein. Spectrum b is the X-band spectrum of 50 mM  $\text{Fe}^{2+}$ -EDTA. Spectra c and d are the respective P-band spectra. Experimental conditions for spectra a–d, respectively: microwave frequencies, 9.13, 9.13, 14.98, 14.98 GHz; microwave powers, 2, 0.01, 6, 0.05 mW; modulation amplitudes, 1, 2.5, 0.8, 0.9 mT; modulation frequency, 100 kHz; temperatures, 11, 8, 23, 13 K. The field scale is appropriate to both X-band and P-band spectra.

have limited ourselves to comparing the signal amplitude with that of a sample of  $\text{Fe}^{2+}$ -EDTA of known concentration. Toward this end we measured the signal intensity of the broad signal from  $\text{Fe}^{2+}$ -EDTA and ferredoxin in the 6–17 K range. The data were fitted to fractional Boltzmann distribution over the two sublevels which suggested  $D$  values of  $1.6 \text{ cm}^{-1}$  for  $\text{Fe}^{2+}$ -EDTA and  $1.3 \text{ cm}^{-1}$  for ferredoxin. However, unpublished magnetic circular dichroism results of M.K. Johnson require that  $D$  have a negative value. It is thus likely that the temperature-dependence of the EPR signal is complicated by relaxation phenomena. Therefore, the fraction of ferredoxin molecules contributing to the broad signal cannot be accurately determined. For a small  $|D|$ , however, the intensities of the spectra recorded at 12 K should have only a small contribution due to population differences of the quintuplet. We found the fraction of contributing ferredoxin molecules to range from 0.6 with a negative  $D$  value to 1.3 for a positive  $D$  value. These rough estimates are consistent with the low-field signal intensity arising from all the reduced ferredoxin molecules.

LeGall et al. [21] observed a similar EPR signal,  $g \approx 11.4$ , from the periplasmic hydrogenase of *Desulfovibrio gigas*; the signal was elicited from a sample which was first reduced by hydrogen then slowly oxidized by protons. Our results suggest that this signal arises from a center having  $S = 2$ , perhaps a  $[3\text{Fe}-n\text{S}]$  cluster, in the hydrogenase.

The signal from the 4Fe cluster which appears on complete reduction shows more spectral features than the maximum of three expected for a magnetically isolated  $S = 1/2$  system. Ohnishi et al. [16] reported this signal to be invariant upon lowering the microwave frequency from 9 to 3 GHz and concluded that the complexity in the signal arose from the existence of different protein conformations. We have now recorded the spectrum of the fully reduced protein at 9 and 15 GHz and have found significant changes, as shown in Fig. 3, particularly in the high-field region of the spectrum. These changes are indicative of some form of magnetic interaction between the integer spin 3Fe center and the  $S = 1/2$  4Fe center.

If the  $S = 1/2$  4Fe cluster is in spin-spin interaction with the  $S = 2$  3Fe cluster, then we can expect effects on the  $S = 1/2$  signal which are

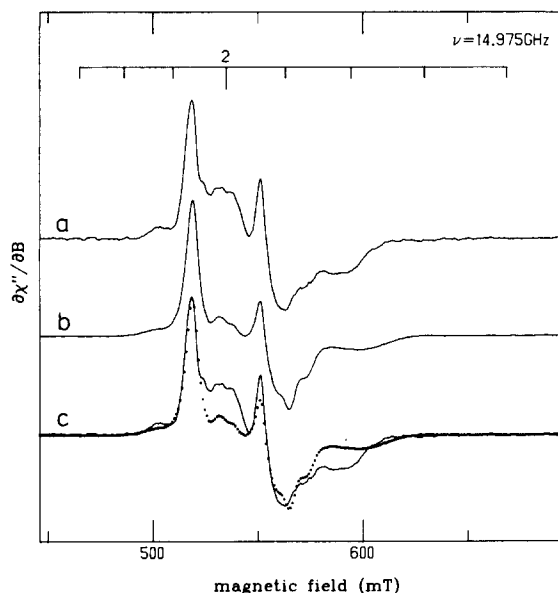


Fig. 3. Frequency dependence of the EPR signal arising from the reduced 4Fe cluster of *T. thermophilus* ferredoxin. Spectra a and b are the P- and X-band EPR spectra, respectively; the field scale is appropriate to the P-band experiment, whereas the g-scale (inset) is common to both. Trace c is an overlay of spectra a and b (the X-band spectrum is dotted). EPR conditions for traces a and b: microwave frequencies, 14975 and 9194 MHz; microwave power, 0.3 and 0.1 mW; modulation amplitudes, 0.8 and 1.2 mT; modulation frequency, 100 kHz; temperatures 23 and 11 K.

analogous to those previously described for 8Fe ferredoxins [11], ubisemiquinone in succinic dehydrogenase [22], and various vitamin B-12-containing enzymes [23]. However, these previous studies were performed on systems in which two different  $S = 1/2$  spin systems were interacting. In the present case, one of the interaction spins is  $S > 1$  and is here assumed to be  $S = 2$ . Therefore, there are important differences in this case compared to previous studies.

Most of these differences derive from the reaction of an integer spin system to an applied magnetic field. We write the Hamiltonian for the  $S = 2$  system as

$$\mathcal{H}_i = g_2 \beta \vec{H} \cdot \vec{S} + D \left[ S_z^2 - S(S+1)/3 + \eta(S_x^2 - S_y^2) \right] \quad (1)$$

where  $g_2$  represents an isotropic  $g$ -tensor, and  $D$  and  $\eta$  are the zero-field splitting parameters [24]. The  $x, y, z$  subscripts refer to the body-frame, or

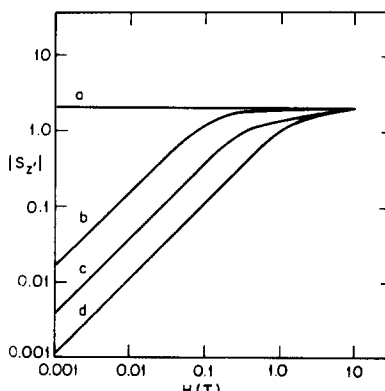


Fig. 4. Variation of the largest value of  $|S_z'|$  for an  $S = 2$  system ( $|D| = 1.4 \text{ cm}^{-1}$ ,  $T = 10 \text{ K}$ ) with the magnitude of applied field at different orientations and values of  $\eta$ . Trace a is for  $\eta = 0$  along  $z$ ; trace b is for  $\eta = 1/3$  along  $x, z$ ; trace c is for  $\eta = 0$  along  $x, y$ ; and trace d is for  $\eta = 1/3$  along  $y$ .

molecular-axes coordinates. By matrix diagonalization methods, we can solve this Hamiltonian for  $|S_z'|$ , the largest moment of the spin system along the  $z'$  direction, i.e., along the applied magnetic field. In Fig. 4 we show the magnitude of  $|S_z'|$  along  $x, y, z$  when  $|D| = 1.4 \text{ cm}^{-1}$  and  $\eta = 0$  or  $1/3$ . If  $\eta$  is not equal to zero, then the  $S = 2$  system has no moment at zero applied field, but a moment is induced in the system as the field is increased. If  $\eta = 0$ , the above is also true except along the spin system  $z$ -axis where the full moment,  $|S_z'| = 2$ , is present regardless of the applied magnetic field. In other words, integer spin systems can appear diamagnetic unless  $g\beta H > D$  except for the 'easy axis' situation when  $\eta = 0$ . (See Ref. 24 for further explanation.) An alternative view of the  $\eta = 0$  case at low applied magnetic field is to envision the spin system as spatially quantized along the  $z$ -axis (body-frame) regardless of the direction of the applied field within the body frame.

If we omit the zero-field terms from the  $S = 2$  Hamiltonian (Eqn. 1), then we can write the electron Zeeman interaction plus the interaction of  $S = 1/2$  with  $S = 2$

$$\mathcal{H} = g_1 \beta H S_{1z'} + g_2 \beta H S_{2z'} - 2J \vec{S}_1 \cdot \vec{S}_2 + \frac{\vec{\mu}_1 \cdot \vec{\mu}_2 - 3(\vec{\mu}_1 \cdot \vec{r})(\vec{\mu}_2 \cdot \vec{r})}{r^3} \quad (2)$$

where  $g_1$  is the projection of the  $G_1$ -tensor along the lab-frame  $z$ -axis,  $g_2$  is an isotropic  $g$  value for an  $S = 2$  system with Eqn. 1 for a Hamiltonian,  $J$  is the scalar exchange coupling constant for the interaction between  $S = 1/2$  and  $S = 2$ , the last term represents the dipole-dipole interaction between the two spin systems, and  $\vec{r}$  is the interatomic unit vector. Normally, both  $S_1$  and  $S_2$  are quantized along the  $z'$  axis, which is very nearly parallel to the lab frame  $z$  axis. This is the situation for the  $S_1$  (spin 1/2) system and also for the  $S_2$  (spin 2) system if  $g_2\beta H \gg D$ .

If  $g_2\beta H < D$  and  $\eta = 0$ ,  $S_2$  will be quantized along some unique axis in body-frame. To clarify this point, we define  $\vec{\mu}_1 \cdot \vec{r}$  or  $g_1\vec{S}_1 \cdot \vec{r}$  as  $\mu_1 r \cos \theta$  where  $\vec{\mu}_1$  is aligned along the applied field direction; therefore,  $\theta$  depends on the particular molecular orientation. However, if  $g_2\beta H < D$  and  $\eta = 0$  then,  $\vec{\mu}_2 \cdot \vec{r}$  can be defined as  $\mu_2 r \cos \psi$  where both  $\vec{\mu}_2$  and  $\vec{r}$  rotate together in the body-frame so that  $\psi$  is a constant for all molecular orientations.

Using the above definitions we can expand Eqn. 1 to first order as

$$\mathcal{H} \approx g_1\beta H \langle S_{1z} \rangle + g_2\beta H \langle S_{2z} \rangle - 2J \langle S_{1z} \rangle \langle S_{2z} \rangle + g_1g_2 \langle S_{1z} \rangle \langle S_{2z} \rangle \frac{(1 - 3 \cos \theta \cos \psi)}{r^3} \quad (3)$$

For the purposes of this discussion, we will ignore the direct EPR transitions from the  $S_2$  system and concentrate only on the transitions from the  $S_1 = 1/2$  system. Subtracting the form of Eqn. 3 with  $\langle S_{1z} \rangle = 1/2$  from that with  $\langle S_{1z} \rangle = -1/2$ , we obtain

$$\Delta E \approx g_1\beta H + \langle S_{2z} \rangle \left[ -2J + g_1g_2 \frac{(1 - 3 \cos \theta \cos \psi)}{r^3} \right] \quad (4)$$

For illustration purposes, we simplify this expression by setting  $\cos \psi$  to zero. Since  $J$ ,  $g_2$  and  $r$  are constants and since  $g_1$  is almost constant, Eqn. 4 can be written as:

$$\Delta E \approx g_1\beta H + b \langle S_{2z} \rangle \quad (5)$$

where  $b$  is a constant. From this expression, one can see that the normal resonance of the spin 1/2 system is split by the various values of  $\langle S_{2z} \rangle$  whether the spin-spin interaction is exchange or

dipole-dipole. Of course, the resonance equation will have a more complicated form if any of the above simplifications are invalid. However, the form of Eqn. 5 is sufficient to explain how the lines in Fig. 3 move with microwave frequency. Referring to Fig. 4, we see that if  $g_2\beta H < D$  and  $\eta = 0$ , then  $\langle S_{2z} \rangle$  is large and constant when the applied magnetic field is along the body frame (zero-field splitting)  $z$ -axis, but has a value proportional to the field when field direction is along the  $x$ - or  $y$ -axis of the body-frame. Thus, if one plots variable frequency EPR data on a  $g$ -scale as in Fig. 3, then one would expect resonances where the applied field is along the  $z$ -axis of the spin 2 system to become closer together as the frequency is increased, as do most weak interaction signals [11,12,22,23] and as occurs along the high field extreme of the signals in Fig. 3. Therefore, one has an indication here that not only is  $\eta$ , the asymmetry parameter of the spin 2 zero-field splitting tensor, near zero, but also the  $z$ -axis of this tensor is along the  $x$ - or  $y$ -axis of the  $G_1$  tensor for the spin 1/2 system.

On the other hand, the low-field 'bumps' on the spectra in Fig. 3 have positions that are independent of microwave frequency, indicating that their Hamiltonians have only field-dependent terms. Again referring to Fig. 4, we see that this is possible along the  $x$ - or  $y$ -axes of the spin 2 tensor; therefore, the  $z$ -axis of the spin 1/2 system probably lies in the  $x$ - $y$  plane of the spin 2 system.

The above arguments, although they lack the rigor that would result from an exact calculation and curve fitting procedure, do provide an explanation for a type of interaction EPR signal. The observation of field-dependent EPR line positions from a spin-spin interaction involving a spin 1/2 protein is probably diagnostic for identifying the interacting spin as an integer spin. This type of spectrum also seems to give structural information such as the alignment of the body frame tensors outlined above. The size of the interaction is around the same magnitude observed previously [11,12,22,23] for interacting spin 1/2 systems, which indicates that the center-to-center distance is probably around 12 Å. We cannot decide from the present information whether the interaction in *Thermus* ferredoxin is exchange or magnetic dipole-dipole in origin.

The results presented above demonstrate two new facts about the  $7\text{Fe}$  from *Thermus*. First, a weak, broad signal at large  $g$  values has been associated with the integer spin multiplet of the reduced  $3\text{Fe}$  cluster. Based on the similarity of this signal to that observed from solutions of  $\text{Fe}^{2+}$ -EDTA, we suggest that this signal is a  $\Delta M = 4$  transition within an  $S = 2$  multiplet. However, integer values of  $S$  greater than 2 cannot be rigorously excluded. This signal may aid in the overall problem of diagnosing the presence of a  $3\text{Fe}$  cluster in a complex protein [25]. Second, we have shown that the complexity in the EPR signal from the reduced  $4\text{Fe}$  center is due to spin-spin interaction with the integer spin of the reduced  $3\text{Fe}$  center, and we offer an explanation for the observation of Ohnishi et al. [16], which indicated that the S-band EPR spectrum of fully reduced protein was the same as the X-band spectrum.

### Acknowledgements

We thank Ms. Carol J. Nettleton for preparation of protein. Financial support is acknowledged from the U.S. Public Health Service, GM 32785 (to R.H. Sands), GM 33806 (M.K.J.), and GM 30974 (J.A.F.).

### References

- Sands, R.H. and Dunham, W.R. (1975) *Q. Rev. Biophys.* 7, 443–504
- Noodleman, L. and Baerends, E.J. (1984) *J. Am. Chem. Soc.* 106, 2316–2327
- Carter, W.C., Kraut, J., Freer, S.T., Alden, R.A., Sieker, L.C., Adman, E. and Jensen, L.H. (1972) *Proc. Natl. Acad. Sci. USA* 69, 3526–3529
- Emptage, M.H., Kent, T.A., Huynh, B.H., Rawlings, J., Orme-Johnson, W.H. and Münck, E. (1980) *J. Biol. Chem.* 255, 1793–1796
- Stout, C.D., Ghosh, D., Patabhi, V. and Robbins, A.H. (1980) *J. Biol. Chem.* 255, 1797–1800
- Huynh, B.H., Moura, J.J.G., Moura, I., Kent, T.A., LeGall, J., Xavier, A.V. and Münck, E. (1980) *J. Biol. Chem.* 255, 3242–3244
- Kent, T.A., Huynh, B.H. and Münck, E. (1980) *Proc. Natl. Acad. Sci. USA* 77, 6574–6576
- Thomson, A.J., Robinson, A.E., Johnson, M.K., Moura, J.J.G., Moura, I., Xavier, A.C. and LeGall, J. (1981) *Biochim. Biophys. Acta* 670, 93–100
- Ghosh, D., Furey, Jr., W., O'Donnell, S. and Stout, C.D. (1981) *J. Biol. Chem.* 256, 4185–4192
- Adman, E.T., Sieker, L.C. and Jensen, L.H. (1973) *J. Biol. Chem.* 248, 3987–3996
- Mathews, R., Charlton, S., Sands, R.H. and Palmer, G. (1975) *J. Biol. Chem.* 249, 4326–4328
- Orme-Johnson, W.H. and Sands, R.H. (1973) in *Iron-Sulfur Proteins*, Vol. II, (Lovenberg, W., ed.), pp. 195–238, Academic Press, New York
- Findling, K.L., Yoshida, T. and Fee, J.A. (1984) *J. Biol. Chem.* 259, 123
- Hille, R., Yoshida, T., Tarr, G.E., Williams, C.H., Ludwig, M.L., Fee, J.A., Kent, T.A., Huynh, B.H. and Münck, E. (1983) *J. Biol. Chem.* 258, 13008–13013
- Stevenson, R.C. (1982) Ph.D. Thesis, The University of Michigan. Available from University Microfilms, Ann Arbor, MI
- Ohnishi, T., Blum, H., Sato, S., Nakazawa, K., Hon-nami, K. and Oshima, T. (1980) *J. Biol. Chem.* 255, 345–348
- Hagen, W.R., Hearshen, D.O., Sands, R.H. and Dunham, W.R. (1985) *J. Magn. Reson.* 61, 220–232
- Hagen, W.R., Hearshen, D.O., Harding, L.J. and Dunham, W.R. (1985) *J. Magn. Reson.* 61, 233–244
- Hagen, W.R. (1982) *Biochim. Biophys. Acta* 708, 82–98
- Hagen, W.R., Dunham, W.R., Sands, R.H., Shaw, R.W. and Beinert, H. (1984) *Biochim. Biophys. Acta* 765, 399–402
- LeGall, J., Ljungdahl, P.O., Moura, I., Peck, Jr., H.D., Xavier, A.V., Moura, J.J.G., Teixeira, M., Huynh, B.H. and DerVartanian, D.V. (1982) *Biochem. Biophys. Res. Commun.* 106, 610–616
- Ruzicka, F.J., Beinert, H., Schepler, K.L., Dunham, W.R. and Sands, R.H. (1975) *Proc. Natl. Acad. Sci. USA* 72, 2886–2890
- Schepler, K.L., Dunham, W.R., Sands, R.H., Fee, J.A. and Abeles, R.H. (1975) *Biochim. Biophys. Acta* 397, 510–518
- Dunham, W.R., Sands, R.H., Shaw, R.W. and Beinert, H. (1983) *Biochim. Biophys. Acta* 748, 73–85
- Orme-Johnson, W.H. and Orme-Johnson, N.R. (1982) in *Iron-Sulfur Proteins* (Spiro, T.G., ed.), pp. 67–96, John Wiley & Sons, New York